Synthesis-Dependent Neurobehavioral and Developmental Effects of Aluminium Oxide Nanoparticles in Zebra fish larvae

[1] Sanskruti Thakur, [2] Shamshad Ather, [1] Mansee Thakur, [1] Shivani Gangani, [1] Rouchelle Shylla, [1] Himanshu Gupta

Corresponding Author: Himanshu Gupta

Abstract: Background: The rising incidence of cognitive disorders, including dementia, underscores the urgent need for cost-effective and ethically compliant animal models to study neurodegenerative mechanisms and evaluate therapeutic strategies. Nano particle-induced neurotoxicity has emerged as a promising approach for modelling cognitive impairment; however, the synthesis route plays a critical role in determining nano particle biocompatibility and toxic potential. Objective: This study compares biologically synthesized aluminium oxide nano particles (bio-Al_2O_3 NPs) with chemically synthesized aluminium oxide nano particles (chem-Al_2O_3 NPs) to establish a safe and reliable cognition-deficit model in zebra fish (Danio rerio).Methods: Al_2O_3 NPs were synthesized via (i) a green method using Citrus aurantium (orange peel) extract and (ii) conventional chemical precipitation. Characterization involved UV-Vis spectroscopy, X-ray diffraction, transmission electron microscopy, Fourier-transform infrared spectroscopy, and elemental analysis. Following Fish Embryo Toxicity (FET) protocols, zebra fish embryos and larva**e were** exposed to graded NP concentrations. Developmental endpoints included survival, hatching success, cardiac function, and morphological defects. Neurobehavioral assays assessed locomotors activity, zone preference, and anxiety-like responses. Results: Bio-Al_2O_3 NPs were spherical (8–25 nm), partially amorphous, and exhibited minimal aluminium release (0.0201 ppm), whereas chem-Al_2O_3 NPs were rod-shaped (8–11 nm), highly crystalline, and contained elevated aluminium levels (6.83 ppm). Chem-Al_2O_3 exposure induced significant developmental toxicity, including pericardial edema, reduced heart rate, and pronounced behavioural impairments. Bio-Al_2O_3 NPs elicited subtle but measurable cognitive disturbances with negligible structural abnormalities. Conclusion: Green-synthesized Al_2O_3 NPs provide a safer alternative for inducing cognition-related phenotypes in zebra fish, offering a sustainable and effective platform for neurotoxicity modelling and therapeutic screening. This work emphasizes the influence of synthesis strategies on nano toxicological outcomes and supports zebra fish as a valuable model for neurobehavioral research.

Key words: (MeSH-based keyword), Aluminium Oxide / toxicity, Zebrafish / developmental toxicity, Larva / adverse effects, Behaviour, Animal / adverse effects, Neurobehavioral Manifestations / toxicity, Dose-Response Relationship

Introduction

Cognitive dysfunction is a broad term encompassing various neurological impairments that negatively affect memory, learning, attention, and decision-making processes [1]. According to Reitz et al. (2011) [2], cognitive deficits are hallmark features of several

neurodegenerative disorders, including Alzheimer's disease, Parkinson's disease, and other forms of dementia. As global life expectancy increases, the prevalence of cognitive impairment is projected to rise sharply, presenting a growing public health burden [3]. Understanding the underlying mechanisms of cognitive decline is essential for developing effective preventive and therapeutic strategies.

While aging is a major contributor, environmental neurotoxins such as heavy metals and engineered nonmaterial's are also implicated in cognitive impairment (Barber et al., 2017) [4]. Aluminium (Al) has emerged as a neurotoxin agent of concern due to its widespread use in industrial and biomedical applications, as well as its potential to disrupt neural function [5]. Aluminium exposure has been linked to oxidative stress, neuron Flammarion, and subsequent cognitive dysfunction [6]. Al accumulation in the brain may interfere with synaptic transmission, enhance oxidative damage, and promote neuronal death, though the mechanisms remain under investigation [7].

The advent of nanotechnology has intensified concerns over the toxicological impacts of aluminium-based compounds, such as aluminium chloride and Al_2O_3 NPs, which are commonly employed in cosmetics, drug delivery systems, catalysis, and environmental remediation [8]. Aluminium chloride demonstrates rapid uptake with severe cognitive impairments, while Al_2O_3 NPs exhibits slower uptake, resulting in subtle but significant cognitive declines. Despite its slower absorption, Al_2O_3 NPs neurodevelopment effects remain concerning, especially in nanoscale formulations. Due to their small size and high surface area, these nano particles can cross biological barriers, including the blood-brain barrier, and exert toxic effects at the cellular and molecular levels [9]. However, the physicochemical properties of nano particles—and hence their biological impact—are strongly influenced by the synthesis method used.

Synthesis technique is a critical determinant of nano particle biocompatibility and toxicity. Green or biological synthesis methods, often using plant extracts, tend to produce nano particles with enhanced stability, reduced toxicity, and biocompatibility due to the presence of natural capping agents [10]. In contrast, chemically synthesized nanop articles may retain toxic residues or have surface properties that heighten oxidative and inflammatory responses in biological systems [11]. For instance, biosynthesized Al_2O_3 NPs are often amorphous and spherical with lower aluminium content, while chemically synthesized variants may be rod-shaped, crystalline, and more reactive—contributing to higher developmental and neurotoxic outcomes [8,12].

The zebrafish (Danio rerio) model has gained prominence in neurotoxicity and cognitive function research due to its transparent embryos, conserved vertebrate neuron atomy, and complex behavioural repertoire [13]. Zebra fish exhibit learning, memory, and exploratory behaviours that are analogous to mammalian models, making them ideal for neurobehavioral assays [14]. Their suitability is further demonstrated by tools like the novel tank test, T-maze, and inhibitory avoidance tasks, which allow for precise behavioural phenol typing [15].

Al_2O_3 NPs have been implicated in cognitive impairments through mechanisms involving oxidative stress, synaptic disruption, apoptosis, and neuro inflammation [12]. Excessive generation of reactive oxygen species (ROS), as seen with chemically synthesized NPs, can lead to lipid per oxidation, mitochondrial dysfunction, and DNA damage [16]. Furthermore, the activation of glial cells and release of pro-inflammatory cytokines exacerbate neuronal injury [17], while disruptions in neurotransmitter systems impair cognitive processing [18].

Given the rising concern about Al_2O_3 NP exposure, this study aimed to compare the cognitive and developmental effects of biologically versus chemically synthesized Al_2O_3 NPs in zebrafish. The goal was to establish a reliable, minimally toxic zebrafish model of cognitive impairment that can serve as a platform for therapeutic screening. Fish embryo toxicity and behavioural endpoints—including locomotor activity and memory—were evaluated.

Ultimately, the findings from this study will contribute to a deeper understanding of nano particle-induced neurotoxicity, promote the development of safer nano materials, and aid in establishing zebra fish as a standard model for cognition-related nano toxicological research. These insights will be pivotal for informing regulatory decisions on nano material usage and safeguarding public health.

Material sand Methods

1. Nanoparticle Synthesis

The study involved two approaches for synthesizing Al_2O_3 nanoparticles:

Biological Synthesis: Al_2O_3 NPs were synthesized using a green synthesis method, which employs biological agents as reducing and stabilizing agents, following the protocol described by Nagarajan et al. (2020) [20]. This environmentally friendly approach emphasized low-temperature synthesis, minimizing energy inputs and promoting sustainable practices. Citrus aurantium fruit peel was procured commercially and authenticated by Dr. Harsh ad M. Pandit, formerly Head and Associate Professor of Botany, G. N. Khalsa College, Mumbai (Authentication number: st P 09245059). Ten grams of the dried and finely ground peel powder were extracted in 100 mL of distilled water. Filtration was performed to remove coarse particulates and impurities, producing a clear solution suitable for nano particle synthesis and subsequent analysis. Five millilitres of this peel extract were mixed with 100 mL of 0.5 M potassium aluminium sulphate solution. Two grams of sodium hydroxide and two grams of zinc acetate solution were added, followed by an additional 4 g of sodium hydroxide to maintain a pH of 12. The mixture was stirred continuously for two hours. After centrifugation at 6000 rpm for 30 minutes, the supernatant was heated for 60 minutes, turning light brown, and yielding pale brown nano particles, which were collected and stored for further analysis (Figure 1) [19].

Chemical Synthesis: Al_2O_3 NPs were synthesized via a chemical precipitation method as described by Bhoi et al. (2018) [21], using aluminium nitrate monohydrate ($Al(NO_3)_3 \cdot 9H_2O$, Sigma-Aldrich) as the precursor and methanol as the solvent. Briefly, 25 g of $Al(NO_3)_3 \cdot 9H_2O$ was dissolved in 75 mL of methanol and magnetically stirred for 30 minutes, yielding a yellow solution (pH 5.9). The pH was then adjusted to 12 by gradual addition of sodium hydroxide (NaOH) and stirred for 1.5 hours. The mixture was centrifuged at 3780 rpm for 30 minutes; the supernatant was discarded, and the precipitate collected. The product was transferred to Petri plates and incubated overnight at 37 °C to obtain dried Al_2O_3 NPs**(Figure 1)**.

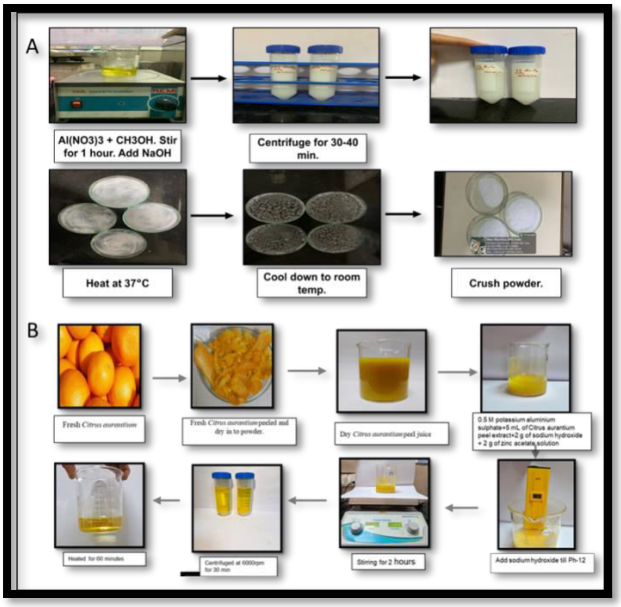

Figure 1: The synthesis method carried out for biological and chemical synthesis **A** - Chemical Synthesis, **B**- Biological synthesis of Al_2O_3 NPs

2. Nano particle Characterization

To confirm the identity, structure, morphology, stability, and elemental composition of the synthesized Al_2O_3 NPs, both biologically and chemically synthesized, a range of analytical techniques were employed. UV–Visible spectroscopy (Epoch, BioTek, USA) was used to evaluate the optical properties and colloidal stability of the nano particles in the 250–700 nm range. X-ray diffraction (XRD) (Empyrean, PAN alytical, The Netherlands) was performed to determine crystalline size, structural characteristics, and phase purity, while Fourier Transform Infrared Spectroscopy (FTIR) (Hyperion 3000 Microscope with Vertex 80 System, Bruker, Germany) was used to identify surface functional groups and bonding characteristics. Transmission Electron Microscopy (TEM) (Tecnai G2 12, FEI, USA) provided detailed insights into particle size, morphology, and surface features, with analysis outsourced to ICON Labs. Energy Dispersive X-ray Spectroscopy (EDX) was used to verify elemental composition, and Inductively Coupled Plasma–Atomic Emission Spectroscopy (ICP–AES) (ARCOS, SPECTRO Analytical Instruments GmbH, Germany) was employed for quantitative

elemental analysis. TEM, XRD, FTIR, and ICP–AES analyses were outsourced for detailed evaluation.

3. Embryo Collection and Maintenance

The study was approved by the Institutional Animal Ethics Committee (IAEC) of MGMIHS and conducted following CPCSEA guidelines to ensure humane care of zebra fish (Danio rerio).

Adult Danio rerio (inbred wild-type) were maintained in a Gendanio (Zebrafish India) automated recalculating aquaculture system at the Zeb Cog Zebra fish Laboratory, MGMIHS, Navi Mumbai. The system was maintained at 28 ± 1 °C with a 14:10 h light/dark photoperiod and pH ~7, with total dissolved solids (TDS) and conductivity regulated according to standard zebrafish husbandry guidelines. Fish were fed live Artemia (OSI Artemia, USA) once daily and commercial pellet food twice daily. For breeding, males and females were separated the evening prior and paired the next morning in breeding tanks. Fertilized embryos were collected post-fertilization, and the developmental stage was confirmed under a stereomicroscope (Carl Zeiss Stemi 305) before experimental exposure (4 hpf). Collected embryos were washed and transferred into 400 mL borosilicate glass beakers containing 250 mL of aerated embryo medium (E3 medium; pH 7.3; Na^+ 3.8 ± 0.06 mg/L; Ca^{2+} 6.96 ± 0.06 mg/L; K^+ 0.45 ± 0.04 mg/L; dissolved oxygen ~97%) and maintained at 28.5 °C. To ensure optimal water quality, 30% of the medium was renewed daily. In accordance with established protocols (Chen et al., 2020; Liu et al., 2018), embryos were not fed until 120 hpf.

4. In Vivo Exposure of Al_2O_3 Nano particles using FET

In vivo toxicity of the synthesized Al_2O_3 NPs was evaluated using the Fish Embryo Toxicity (FET) test according to OECD Test Guideline 236. Hundred zebra fish embryos (n = 10 per concentration) were used, including a control group (0 µg/mL) and treatment groups exposed to Al_2O_3 NPs at concentrations of 1,2,4,6,8,9,10,11,12µg/mL until 120 hpf (5 dpf). Fish water, prepared in accordance with Annex 2 of OECD 236, was used as the exposure medium and maintained within the following ranges: pH 7.5–8.0, conductivity 632–676 µS/cm², hardness 217–235 mg/L $CaCO_3$, and dissolved oxygen 92–98%. Immediately after egg collection, embryos at 4 hpf were randomly distributed into 12-well culture plates, with 5 embryos per well containing 2 mL of nano particle suspension. The embryos were maintained at 28 ± 0.5 °C under a 14 h light/10 h dark photoperiod, and the test solutions were renewed every 24 h to ensure consistent exposure. This setup enabled high-throughput testing with minimal manipulation of embryos. Developmental parameters, including survival, hatching rate, and morphological abnormalities were assessed daily under a Carl Zeiss Stemi 305 stereomicroscope, and images were documented for analysis.

5. Behavioural Analysis of Larvae

Post exposure, at 5 dpf, zebrafish larvae from each treatment group was subjected to behavioural assessments to evaluate the neuro developmental effects of Al_2O_3 NP exposure. Individual larvae were placed in 24-well plates and acclimatized for 10 minutes before testing. All behavioural recordings were conducted during the light phase (9:00 AM–5:00 PM) to minimize circadian variability, using an automated video tracking system (View Point Life Sciences, France) for data acquisition and analysis. Behavioural endpoints measured included swimming speed (total distance moved per unit time, mm/s), exploratory behaviour (time spent in central vs. peripheral zones, indicative of anxiety or stress), and darting behaviour (frequency of sudden, rapid movements suggestive of hyper reactivity or escape responses). Data were quantitatively analysed and compared across treatment groups to determine dose-dependent neurobehavioral impacts of Al_2O_3 NPs exposure.

Results

1. Nanoparticle Characterization

Al_2O_3 NPs were successfully synthesized using both chemical and biological approaches, and their formation was confirmed through a series of spectroscopic and microscopic analyses.

UV–Vis spectroscopy of chem-Al_2O_3 NPs revealed a strong absorption peak at 230 nm, consistent with previously reported absorbance for Al_2O_3 (230–250 nm). The nanoparticles maintained optical stability over a four-week monitoring period (Figure 2). The optical band gap, calculated from Tauc's plot, was 5.39 eV (Figure 3), in agreement with reported indirect band gap values ranging from 5.25 to 5.51 eV. In contrast, Bio-Al_2O_3 NPs displayed a characteristic absorption peak at 360 nm, which remained stable for four weeks (Figure 2). The band gap estimated from the Tauc plot was 6.22 eV (Figure 3), slightly lower than the bulk Al_2O_3 value (~8.7–9.0 eV) but within the expected nanoscale range, most likely due to quantum confinement effects and the influence of bio-organic compounds from Citrus aurantium extract.

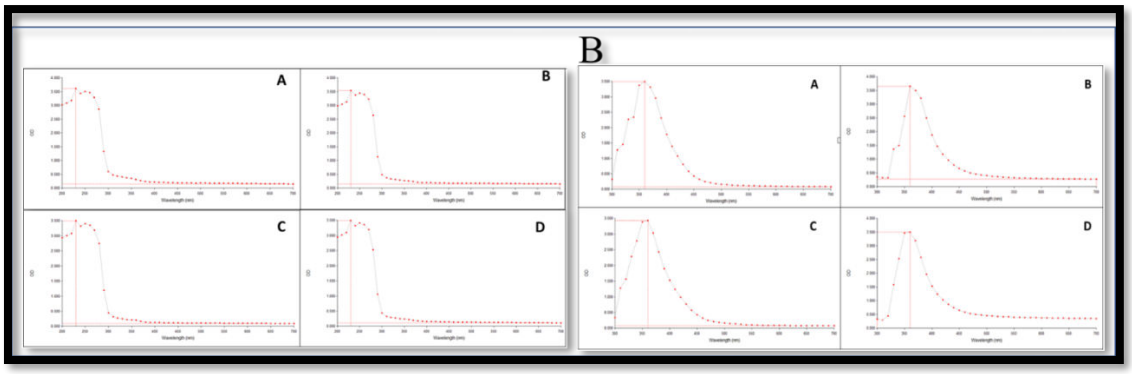

Figure 2: Absorption peaks over a 4-week period for the chemically synthesized nps - **A**- UV-Vis spectrum showing absorbance maximum at 230 nm indicative of presence of

Aluminum oxide and its stability over a period of one month (A-week one, B- Week two, C-Week three and D-Week four), **B**- UV-Vis spectrum showing absorbance maximum at 360 nmindicative of presence of Aluminum oxide and its stability over a period of one month (A-week one, B- Week two, C-Week three and D-Week four

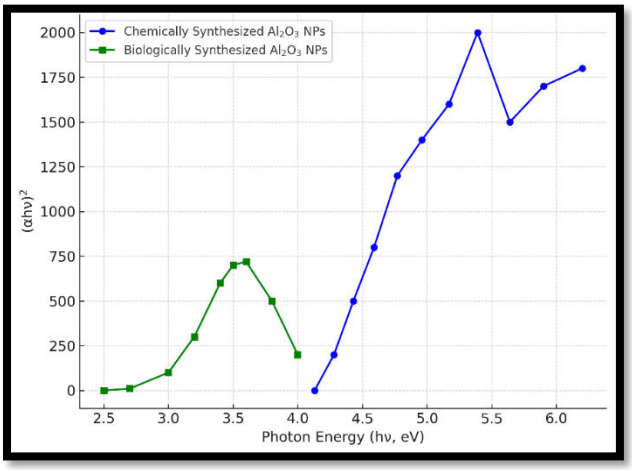

Figure 3: (F): Comparative Tauc plots of chemically and biologically synthesized Al_2O_3 nanoparticles.The optical band gap was estimated by extrapolating the linear region of the $(\alpha h\nu)^2$ vs. hν curve. Chem-Al_2O_3 nanoparticles showed a band gap in the range of 4.1–6.2 eV, while bio-Al_2O_3 nanoparticles exhibited a higher and more defined band gap of approximately 6.22 eV. These differences highlight the impact of the synthesis route on the optical properties of Al_2O_3 nanoparticles

Morphological evaluation by TEM showed distinct differences between the two synthesis methods. Chem Al_2O_3 NPs were elongated with a rod-like morphology, ranging from 8–11 nm in size (Figure 4A & C). In contrast, biosynthesized nano particles were predominantly spherical with a broader size distribution of 8–25 nm, displaying uniform morphology and dispersion (Figure B & D).

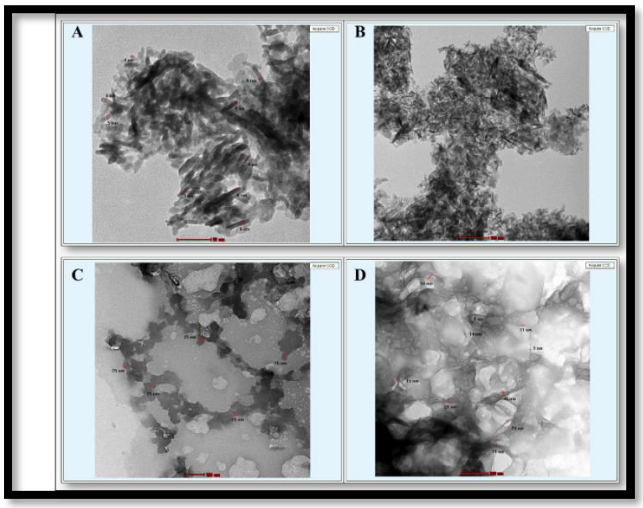

Figure 4: TEM micrographs of chemically and biologically synthesized Al_2O_3 nano particles. (A–B) Chemically synthesized Al_2O_3 NPs showing predominantly aggregated,

irregular clusters of elongated with a rod-like morphology with particle sizes in the range of 4–8 nm, indicating fine crystalline domains with a tendency toward agglomeration. (C–D) Biologically synthesized Al_2O_3 NPs revealing larger, more dispersed spherical and polyhedral particles with sizes ranging from 11–75 nm. The bio-mediated synthesis resulted in relatively well-defined morphology but broader particle size distribution compared to the chemically synthesized nano particles.

XRD analysis further confirmed the structural variations. Chemically synthesized NPs exhibited sharp diffraction peaks corresponding to crystalline aluminium oxide phases, with an average crystallite size of 16.6 nm calculated using the Debye-Scherer equation (Figure 5A). Biosynthesized nano particles, however, displayed a broad diffraction pattern in the 2θ range of 20°–40°, indicative of an amorphous or nano crystalline nature (Figure 5B).

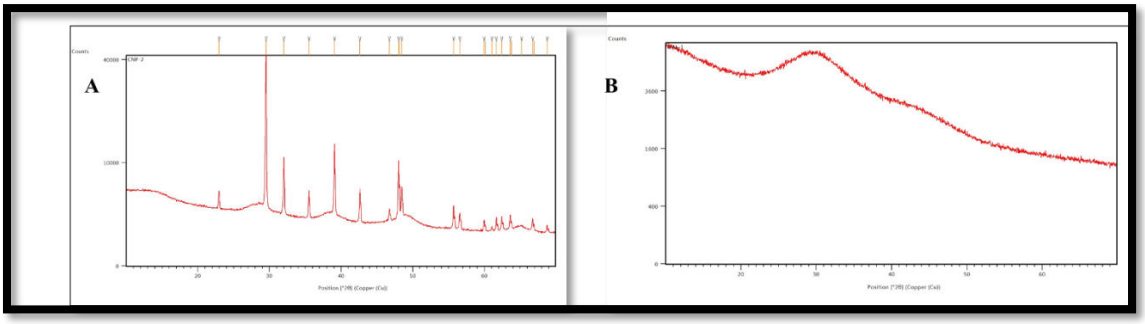

Figure 5: The XRD pattern for chemically synthesized NPs revealed predominantly crystalline αα-Alumina which matches the standard pattern for αα-Alumina (Alpha-alumina –which is a white, puffy powder that is a phase of aluminum oxide, also known as alumina whereas the XRD findings of the biologically synthesized indicated an amorphous or nano crystalline γ-Al_2O_3 structure with minimal crystallization due to low-temperature synthesis.

FTIR spectroscopy confirmed the presence of functional groups in both types of nano particles. In chem-Al_2O_3, peaks corresponding to O–H stretching (3487 cm^{-1}), C–H stretching (2923 cm^{-1}), C=O stretching (1707 and 1633 cm^{-1}), and Al–O vibrations (632–565 cm^{-1}) were observed (Figure 6A). Bio-Al_2O_3 nano particles exhibited characteristic O–H stretching around 3400 cm^{-1}, H–O–H bending near 1630 cm^{-1}, and Al–O stretching and bending vibrations in the 1100–600 cm^{-1} region (Figure 6B), supporting successful nano particle formation mediated by Citrus aurantium peel extract.

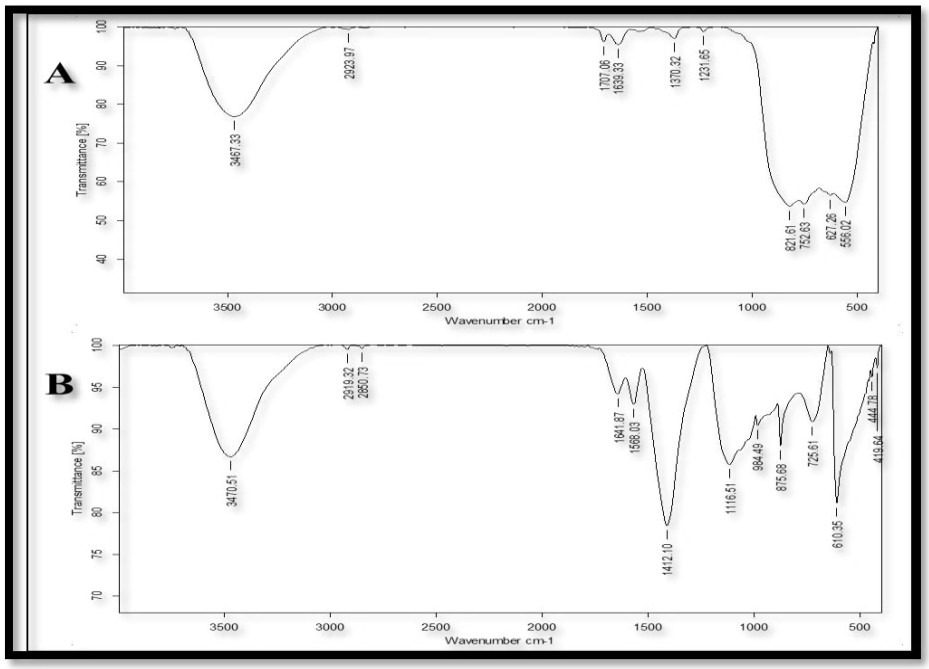

Figure 6: FTIR spectra of Al_2O_3 NPs: (A) chemically synthesized and (B) biologically synthesized. Spectrum A shows O–H stretching (~3467 cm^{-1}), C–H stretching (2923 cm^{-1}), carbonyl/–OH vibrations (1707–1639 cm^{-1}), and a strong Al–O band at 562 cm^{-1}, indicating residual precursor groups with lattice formation. Spectrum B exhibits O–H stretching (~3470 cm^{-1}), amide I and II bands (1641, 1568 cm^{-1}), C–N/C–O vibrations (1412–984 cm^{-1}), and characteristic Al–O stretching (610–444 cm^{-1}), confirming bio molecule-mediated reduction and stabilization.

Elemental analysis by ICP–AES confirmed the purity of both nanoparticle types. Chemically synthesized Al_2O_3 NPs contained aluminium at 6.83 ppm with no detectable heavy metal contamination (Table 1 – CAL-3). Biosynthesized nanoparticles showed aluminium content of 0.0201 ppm, while barium, copper, tin, iron, cadmium, lead, and mercury were below detection limits (Table 1- OAL 1& 2).

Sample	Ba	Cu	Sn	Fe	Al	Cd	Pb	Hg
	ppm	ppm	ppm	ppm	ppm	ppm	ppm	ppm
OAL-1	0.0201	ND	ND	0.249	>120	ND	ND	ND
OAL-2	0.0188	ND	ND	0.285	>120	ND	ND	ND
CAL-3	0.0159	ND	ND	0.283	>120	ND	ND	ND
Control	0.0186	ND	ND	0.276	0.0322	ND	ND	ND

Table 1.ICP analysis of Al_2O_3 NPs synthesized by different methods versus control. Elemental concentrations (ppm) are shown. OAL-1, OAL-2 = biologically synthesized; CAL-3 = chemically synthesized; Control = reference. ND = not detected. High Al (>120 ppm) confirmed nanoparticle formation, with only trace Ba and Fe (environmental background). No toxic heavy metals (Cd, Pb, Hg, Sn, Cu) were detected.

Overall, these results demonstrate that while chemically synthesized Al_2O_3 NPs exhibit rod-shaped crystalline structures with high aluminium content and stability, biosynthesized NPs are spherical, nanocrystalline to amorphous in nature, and stabilized by phytochemicals from Citrus aurantium extract. Both synthesis routes successfully produced Al_2O_3 NPs with distinct physicochemical properties that may influence their biological applications.

2. FET result

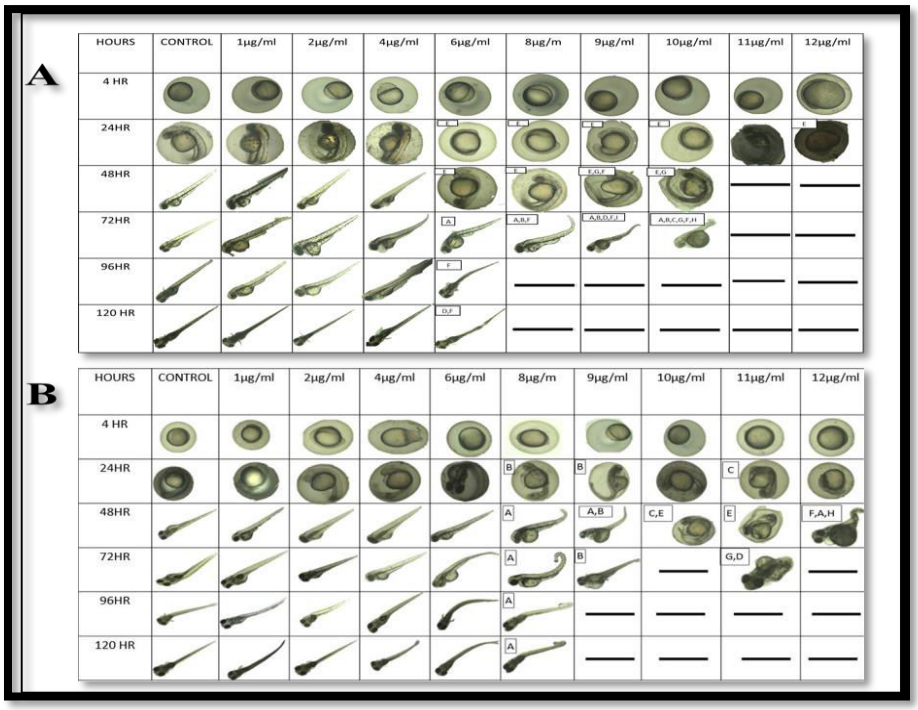

Figure 7: **A**- Bio-Al203 np exposure - A-Pericardial Edema, B-edema, C-Notochord Defects, D-Curved Body Axis, E-Delayed hatching, F- Lordosis, G-Scoliosis, H-Tail Deformities,
B - Chem-Al203 np exposure - A-Curved Body Axis, B-brain region appears swollen , C-Notochord Defects, D- Eye Deformity, E-Delayed hatching, F-Tail Deformities, G-Pericardial Edema,

The fish embryo toxicity assay revealed a dose-dependent effect of Al_2O_3 NPs on zebra fish embryonic development. In embryos exposed to Chem- Al_2O_3 NP's, (Figure 7A) no significant developmental abnormalities were observed at concentrations ≤4 µg/mL, with normal morphology and hatching comparable to controls. However, at 6 µg/mL, delayed hatching and early signs of developmental stress were evident. A pronounced increase in lethality was observed at 8 µg/mL, corresponding to LC_{50} at 24 hpf, accompanied by multiple morphological malformations. At concentrations ≥9 µg/mL, severe developmental defects were consistently recorded, including a curved body axis, swollen brain region, notochord defects, ocular malformations, tail abnormalities, and

pronounced pericardial edema. These results suggest that chem-Al_2O_3 NPsexert profound toxicity, affecting neural, ocular, cardiac, and musculoskeletal development.
In contrast, embryos exposed to bio-Al_2O_3 NPs(Figure 7B) showed comparatively lower toxicity at moderate doses. Up to 4 µg/mL, no significant abnormalities were observed. At 6 µg/mL, a subset of embryos displayed delayed hatching and mild pericardial edema, with progressive abnormalities noted at higher concentrations. LC_{50} was recorded at 9 µg/mL, indicating a slightly higher tolerance compared to the chemically synthesized counterparts. At ≥10 µg/mL, embryos developed severe deformities, including pericardial edema, generalized edema, notochord defects, body curvature, lordosis, scoliosis, and tail malformations. At 11–12 µg/mL, a significant proportion of embryos appeared collapsed or irregularly shaped, indicative of extreme developmental toxicity.
Comparative analysis indicates that while both types of nanoparticles induce concentration-dependent embryo toxicity (Figure 8,9&10), chem-Al_2O_3 nanoparticles are more detrimental, with an earlier onset of lethality (LC_{50} at 8 µg/mL) and broader multi-organ effects, including brain and ocular malformations. Biologically synthesized nanoparticles exhibited relatively delayed lethality (LC_{50} at 9 µg/mL) and toxicity largely restricted to cardiac and skeletal abnormalities, likely due to the presence of bimolecular capping agents conferring partial protection. Collectively, these findings support the safer toxicological profile of boil-Al_2O_3 nanoparticles, making them more suitable candidates for biomedical applications.

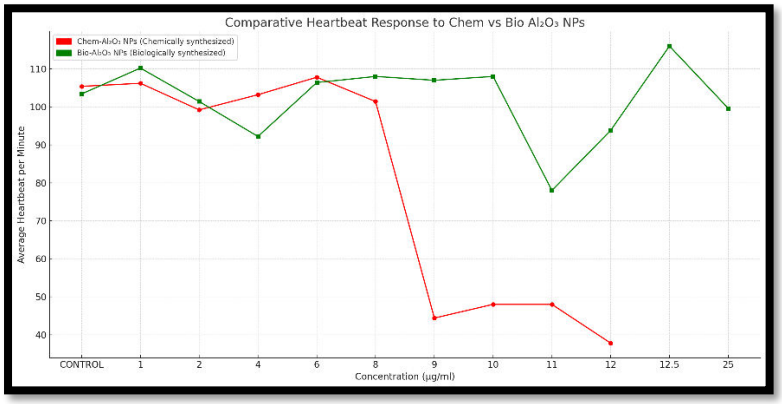

Figure 8: Comparative heartbeat response of zebrafish larvae following exposure to chemically synthesized (Chem-Al_2O_3 NPs) and biologically synthesized (Bio-Al_2O_3 NPs) aluminium oxide nanoparticles across different concentrations (µg/ml). The average heartbeat per minute (calculated over 24–120 h post-exposure) is plotted. Chem-Al_2O_3 NPs (red line) induced a sharp decline in cardiac activity at higher concentrations (≥9 µg/ml), with near-lethal effects observed by 12 µg/ml. In contrast, Bio-Al_2O_3 NPs (green line) maintained relatively stable heartbeat rates even up to 25 µg/ml, indicating greater biocompatibility and reduced cardiotoxicity.

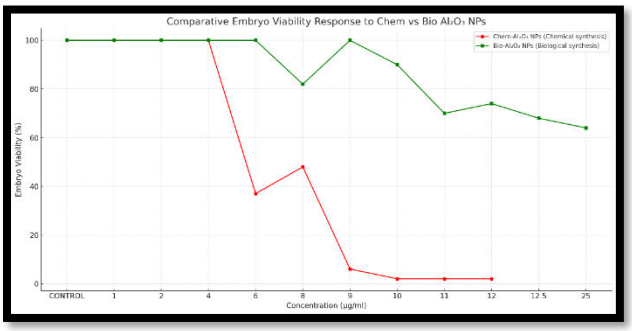

Figure 9: Embryo viability of zebrafish (Danio rerio) following exposure to chemically synthesized (Chem-Al_2O_3 NPs) and biologically synthesized (Bio-Al_2O_3 NPs) aluminium oxide nanoparticles over 24–120 hours post-fertilization. Chem-Al_2O_3 NPs (left) caused a sharp and concentration-dependent reduction in embryo survival, with complete lethality observed from 9 µg/ml onward. In contrast, Bio-Al_2O_3 NPs (right) exhibited higher tolerability, with embryos maintaining >80% viability up to 8 µg/ml and showing gradual decline only at higher concentrations (≥10 µg/ml). The comparative trend highlights the reduced embryotoxicity and greater biocompatibility of biologically synthesized nanoparticles.

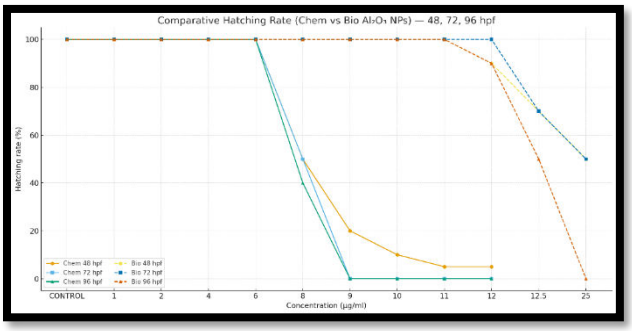

Figure 10: hatching rate of zebrafish embryos following exposure to chemically synthesized (Chem-Al_2O_3 NPs) and biologically synthesized (Bio-Al_2O_3 NPs) aluminium oxide nanoparticles. The average hatching percentage (calculated across 48, 72, and 96 hours post-fertilization) is plotted against increasing concentrations (CONTROL–25 µg/ml). Chem-Al_2O_3 NPs (red line) showed a sharp decline in hatching rates from 8 µg/ml onward, with complete inhibition by 9–12 µg/ml. In contrast, Bio-Al_2O_3 NPs (green line) maintained high hatching rates across most concentrations, with only gradual reductions at ≥12 µg/ml. This trend highlights the reduced embryotoxicity and improved compatibility of biologically synthesized nanoparticles compared to their chemically synthesized counterparts.

3. Behavioural Responses of Zebrafish Larvae to Chemically and Biologically Synthesized Al_2O_3 Nanoparticles:

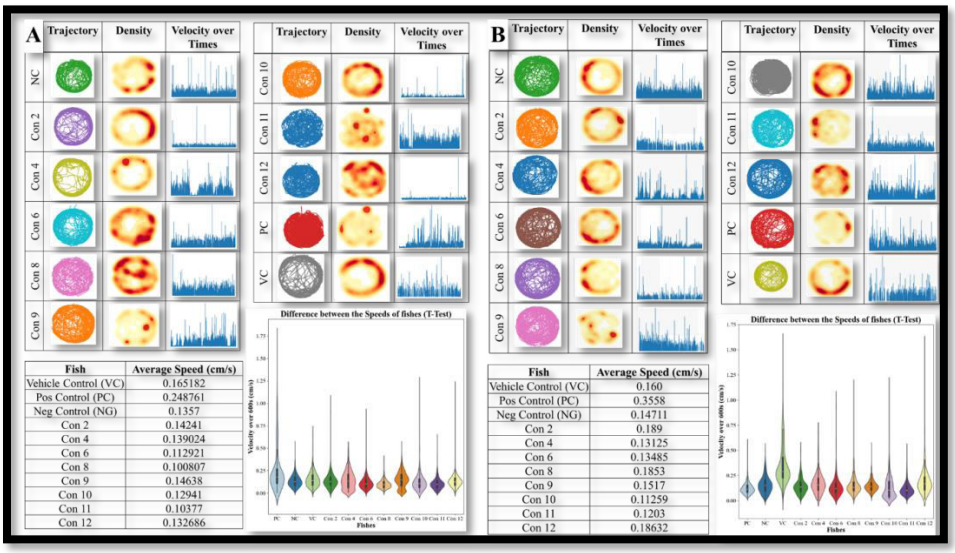

Figure 11: Behavioural analysis of zebrafish larvae exposed to Al_2O_3 nanoparticles synthesized by chemical (A) and biological (B) methods. Locomotor traces, heat maps of spatial occupancy, and velocity profiles illustrate the behavioural responses of larvae across different nano particle concentrations.
(A) Chem-Al_2O_3 NPs: At lower concentrations (0.78–3.125 µg/ml), swimming activity and exploration remain comparable to controls. At higher concentrations (12.5 and 25 µg/ml), larvae display reduced average speed, restricted trajectories, and increased inactivity, reflected by sharper declines in velocity distribution (violin plots).**(B) Bio-Al_2O_3 NPs:** Larvae maintain near-normal exploration and locomotion at low to moderate concentrations (0.78–6.25 µg/ml), with trajectories resembling controls. At higher concentrations (12.5 and 25 µg/ml), reductions in speed and exploration become evident, though the decline is less abrupt than in chemically synthesized groups. Violin plots confirm significant suppression of velocity only at the highest concentrations. Together, the results highlight a stronger neurobehavioral toxicity of chemically synthesized nanoparticles compared to biologically synthesized nano particles.

The study analysed the behaviour of zebrafish larvae exposed to chemically and biologically synthesized Al_2O_3 NPs. The Figure 11 A & B shows that these two nanoparticles exhibited different patterns of neurobehavioral effects.
In the chemically synthesized nanoparticle group (Figure 11A), larvae showed a relatively straightforward dose-dependent suppression of behaviour. At lower concentrations, swimming activity was close to that of the vehicle control, with trajectories extending across the well and density maps displaying dispersed occupancy. However, as concentrations increased, movement became restricted and fragmented. By the time larvae were exposed to 12.5 and 25 µg/ml, their trajectories were noticeably restricted, with swimming restricted to small loops or peripheries,

suggesting a clear reduction in exploratory nature. This suppression was further confirmed by velocity-time traces. Similar to vehicle control, the variations were visible at lower doses with brief pauses in between bouts of locomotor activity. But at higher concentrations these traces flattened out and only displayed weak, sporadic movements during prolonged inactivity. The violin plots also showed this decline as they dropped downward and contracted showing sharp declines in average speeds.

The biologically synthesized nanoparticle group presented a far more heterogeneous profile (Figure 11B). At baseline, larvae in the negative and vehicle controls again showed comparable trajectories to those in the chemical group, with the vehicle control producing slightly elevated activity relative to pure medium. The positive control behaved differently, showing markedly increased average speeds of 0.356 cm/s, more than double the vehicle control, consistent with overstimulation by Donepezil and reflective of deteriorative stress responses rather than genuinely improved motility. There was a greater variability among test concentrations as well. In addition to maintaining normal levels of exploration, larvae at specific concentrations, i.e., Con 2 (0.189 cm/s), Con 8 (0.185 cm/s), and Con 12 (0.187 cm/s) outperformed the vehicle control. Their paths were wide-ranging and intricate; heat maps revealed widely distributed occupancy, suggesting a desire to investigate the full well. The velocity-time profiles of these groups were very dynamic, exhibiting recurrent activity bursts and oscillating patterns that persisted for the duration of the observation. These patterns suggest that biologically generated nanoparticles may enhance locomotor resilience or even show mild stimulatory effects at specific dose.

The comparative analysis between the two treatments underscored these distinctions. In the chemical group, suppression was consistent, predictable, and largely monotonic with concentration. There was no evidence of enhanced behaviour at any dose; rather, all test groups fell at or below the activity levels of the controls, with higher concentrations producing the steepest declines. A more complex interaction between nanoparticles and the larval nervous system may be the cause of the behavioural differences shown in the biological group. This interaction permits resilience at lower to moderate levels until suppression eventually appears at greater exposures.

The study concludes by pointing out a basic difference between the neurobehavioral effects of Al2O3 NPS produced chemically and those produced biologically. The biological preparation provides responses ranging from protection to suppression depending on dose. Whereas the chemical preparation has a consistent toxicological profile marked by gradual motor inhibition. This finding is well supported by the combination of locomotors traces, density maps, velocity-time profiles, and average speed measures.

Discussion

The present study demonstrates that the method of synthesis significantly influences the physicochemical characteristics and biological responses of Al_2O_3 NPs. Chem-

Al_2O_3 NPs were rod-shaped, crystalline, and exhibited a narrower band gap (5.39 eV), while biologically synthesized NPs using *Citrus aurantium* extract were spherical, nano crystalline to amorphous, and displayed a slightly wider band gap (6.22 eV). These observations are consistent with previous studies showing that bio-mediated synthesis often results in nanoparticles capped with phytochemicals, imparting distinct optical and structural properties [22]; [23]. The broader size distribution and amorphous features of bio-Al_2O_3 NPs may be attributed to bio molecule interactions during nucleation and stabilization, as reported earlier for green-synthesized ZnO nanoparticles [24].

Toxicological assessment in zebrafish embryos revealed a clear difference between the two nanoparticle types. Chem-Al_2O_3 NPs induced severe developmental toxicity, with LC_{50} observed at 8 µg/mL, leading to neural, ocular, cardiac, and musculoskeletal malformations. In contrast, bio-Al_2O_3 NPs displayed comparatively reduced toxicity, with LC_{50} recorded at 9 µg/mL and deformities largely restricted to cardiac and skeletal tissues. This aligns with reports that plant-mediated nanoparticles often show improved biocompatibility due to surface capping by organic residues that modulate toxicity [25]; [26]. Furthermore, studies on mammalian systems also indicate that surface modifications by biological extracts reduce nanoparticle-induced cytotoxicity [25].

Cardiac function, accessed via heart rate, further emphasized these differences. Chem-Al_2O_3 NPs caused a sharp decline in heartbeat rates above 9 µg/mL, while Bio-Al_2O_3 NPs maintained near-normal cardiac activity up to higher concentrations. These results mirror earlier findings where nanoparticle-induced pericardial edema and bradycardia in zebrafish embryos were linked to oxidative stress and ion channel disruption [27]; [28]. The reduced cardiotoxicity of biosynthesized particles indicates a protective role of phytochemical capping, which may attenuate reactive oxygen species (ROS) generation, as also highlighted in other nanotoxicology studies [26].

Behavioural analysis of zebra fish larvae provided additional insight into neuro developmental effects. Chem-Al_2O_3 NPs induced a dose-dependent suppression of locomotion, consistent with neurotoxicity and impaired motor coordination. Conversely, Bio-Al_2O_3 NPs demonstrated a heterogeneous response, with some doses even enhancing exploratory behaviour before eventual suppression at higher concentrations. This biphasic effect suggests that photochemical coatings may modulate nanoparticle–nervous system interactions, possibly by influencing neurotransmitter pathways or synaptic activity. Similar hormetic behavioural responses have been observed in zebrafish exposed to green-synthesized silver and titanium dioxide nanoparticles [29]; [30].

Collectively, these findings highlight that nanoparticle synthesis routes critically affect not only structural and optical properties but also biological safety. Chemically synthesized Al_2O_3 NPs exhibit consistent toxicological effects, whereas biologically synthesized counterparts show comparatively reduced embryo toxicity, cardiotoxicity,

and neurobehavioral suppression. This emphasizes the potential of green synthesis in generating safer nanomaterials for biomedical applications, particularly in drug delivery and therapeutic platforms. Future studies should investigate the molecular pathways underlying these protective effects, with emphasis on oxidative stress, apoptosis, and transcriptomic alterations in zebrafish models [23].

Conclusion

This study demonstrates that the synthesis method critically influences both the physicochemical features and biological responses of Al_2O_3 NPs. Chem-Al_2O_3 NPs were crystalline and rod-shaped, displaying high aluminium content and strong embryo toxic, cardio toxic, and neurobehavioral effects in zebrafish. In contrast, bio-Al_2O_3 NPs derived from *Citrus* aurantium extract were spherical, partially amorphous, and exhibited reduced developmental toxicity, milder cardiac effects, and moderate but detectable behavioural and cognitive alterations. The relatively safer profile of bio-Al_2O_3 NPs can be attributed to phytochemical surface capping, which likely attenuates oxidative stress–mediated damage. Collectively, these findings highlight the potential of biologically synthesized Al_2O_3 NPs as an eco-friendly and biocompatible tool for inducing cognition-related phenotypes in zebra fish, providing a reliable and ethically sound model for neurotoxicity studies and therapeutic screening.

Abbreviations

Al_2O_3 NPs - Aluminium oxide nanoparticles
bio-Al_2O_3 - Biologically synthesized Aluminium oxide nanoparticles
chem-Al_2O_3 - Chemically synthesized Aluminium oxide nanoparticles
XRD - X-ray diffraction
TEM - transmission electron microscopy
FTIR - Fourier-transform infrared spectroscopy
FET - Fish Embryo Toxicity
NaOH - sodium hydroxide
TDS - Total dissolved solids

Funding: The authors declare that this study was conducted without any financial support or funding from external sources.

Author Contributions

ST: Methodology, Investigation, Data Curation, Formal Analysis, Visualization, Writing – Original Draft.
SA: Methodology, Investigation, Validation, Formal Analysis, Writing – Review & Editing.
MT: Conceptualization, Supervision, Project Administration, Writing – Review & Editing.

SG: Investigation, Resources, Data Curation, Visualization.
RS: Investigation, Resources, Visualization, Writing – Review & Editing.
HG: Conceptualization, Supervision, Methodology, Formal Analysis, Writing – Original Draft, Writing – Review & Editing, Corresponding Author.

Conflict of interest: The authors declare no conflict of interest financial or otherwise.

Acknowledgments: The authors sincerely thank CRL Lab, MGMSBS, MGMIHS, for providing essential infrastructure. We also extend our gratitude to the Sophisticated Analytical Instrument Facility (SAIF) for granting access to advanced analytical instrumentation, enabling related student studies at subsidized rates.

Author Address

[1] Department of Medical Biotechnology, Central Research Laboratory, MGM School of Biomedical Sciences, Mahatma Gandhi Mission Institute of Health Sciences, Kamothe, Navi Mumbai, Maharashtra, India
[2] Research Associate, MGM Medical College, Nerul West, Navi Mumbai - 400706, Maharashtra, India
[1] Professor, Department of Medical Biotechnology, Central Research Laboratory, MGM School of Biomedical Sciences, Mahatma Gandhi Mission Institute of Health Sciences, Kamothe, Navi Mumbai, Maharashtra, India
[1] PG Student, Department of Medical Biotechnology, Central Research Laboratory, MGM School of Biomedical Sciences, Mahatma Gandhi Mission Institute of Health Sciences, Kamothe, Navi Mumbai, Maharashtra, India
[1] Associate Professor, Department of Medical Biotechnology, Central Research Laboratory, MGM School of Biomedical Sciences, Mahatma Gandhi Mission Institute of Health Sciences, Kamothe, Navi Mumbai, Maharashtra India

References

1. Swerdlow RH. The neurodegenerative mitochondriopathies. J Alzheimers Dis. 2020;78(1):39–55
2. Reitz C, Brayne C, Mayeux R. Epidemiology of Alzheimer disease. Nat Rev Neurol. 2011;7(3):137–52
3. Prince M, Wimo A, Guerchet M, Ali GC, Wu YT, Prina M. World Alzheimer Report 2015: The Global Impact of Dementia. London: Alzheimer's Disease International; 2015
4. Barber RC, Lam HF, Javed A, Porter NR, Fisher A, Beresford MW. Metal exposure and neurodegenerative disease: Epidemiology and mechanisms. Neurosci Lett. 2017; 639:68–78.

5. Bondy SC. Low levels of aluminium can lead to behavioural and morphological changes associated with Alzheimer's disease and age-related neuro degeneration. Neuro toxicology. 2016;52:222–9.
6. Exley C. Aluminum should now be considered a primary etiological factor in Alzheimer's disease. J Alzheimers Dis Rep. 2017;1(1):23–5.
7. Kumar V, Gill KD. Aluminium neurotoxicity: Neurobehavioural and oxidative aspects. Arch Toxicol. 2020;94(3):740–58.
8. Kumari M, Khan SS, Pakrashi S, Mukherjee A, Chandrasekaran N. Cytogenetic and genotoxic effects of aluminum oxide nanoparticles on human lymphocytes in vitro. Environ Sci Technol. 2014;48(10):6121–9.
9. Sadegh S, Mortazavi SM, Rezayat SM, Shahverdi AR. The role of physicochemical properties of nanoparticles in their toxicity. Nanomed J. 2015;2(1):1–12.
10. Iravani S. Green synthesis of metal nanoparticles using plants. Green Chem. 2011;13(10):2638–50.
11. Kharissova OV, Dias HR, Kharisov BI, Pérez BO, Pérez VMJ. The greener synthesis of nanoparticles. Trends Biotechnol. 2013;31(4):240–8.
12. Hussain S, Al-Nsour F, Rice AB, Marshburn J, Yingling B, Ji Z, et al. Comparative neurotoxicity of chemically and biologically synthesized nanoparticles: role of synthesis pathway in toxicity. Nanotoxicology. 2019;13(9):1232–48.
13. Kalueff AV, Stewart AM, Gerlai R. Zebrafish as an emerging model for studying complex brain disorders. Trends Pharmacol Sci. 2014;35(2):63–75.
14. Gerlai R. Learning and memory in zebrafish (Danio rerio). Methods Cell Biol. 2016;134:551–86.
15. Stewart AM, Gaikwad S, Kyzar E, Green J, Roth A, Kalueff AV. Modeling anxiety using adult zebrafish: a conceptual review. Neuropharmacology. 2012;62(1):135–43.
16. Lushchak VI. Environmentally induced oxidative stress in aquatic animals. Aquat Toxicol. 2011;101(1):13–30.
17. Heneka MT, Golenbock DT, Latz E. Innate immunity in Alzheimer's disease. Nat Immunol. 2015;16(3):229–36.
18. Jin Y, Wu S, Zeng Z, Fu Z. Effects of environmental pollutants on gut microbiota. Environ Pollut. 2019;248:833–46.
19. Rao N, Kumar A, Sharma S. Green synthesis of aluminum oxide nanoparticles using Citrus aurantium extract and their antimicrobial activity. J Nanostruct Chem. 2021;11:123–34.
20. Nagarajan S, Priyadharshini S, Kalpana R. Plant-mediated synthesis of metal oxide nanoparticles: Eco-friendly approach and applications. Mater Today Proc. 2020;33:2922–8.
21. Bhoi P, Patel R, Kumar V. Chemical precipitation method for the synthesis of aluminum oxide nanoparticles and characterization. Mater Sci Eng B. 2018;230:34–42.

22. Ahamed, M. (2010). Toxic response of nickel nanoparticles in human lung epithelial cells. Toxicology in Vitro, 24(4), 1052–1058.
23. Asharani, P. V., Wu, Y. L., Gong, Z., &Valiyaveettil, S. (2008). Toxicity of silver nanoparticles in zebrafish models. Nanotechnology, 19(25), 255102.
24. Mohanasundaram P, Saral A M. Binding properties and biological applications of green synthesized ZnO nanoparticles from neem flower. Scientific Reports. 2025 May 22;15(1):17727..
25. Chen, T. H., Lin, C. Y., & Tseng, M. C. (2011). Behavioral effects of titanium dioxide nanoparticles on larval zebrafish (Danio rerio). Marine Environmental Research, 72(1–2), 49–55.
26. Gao, J., & Feng, S. S. (2013). Effects of nanoparticles on cardiac physiology in zebra fish embryos. Nano toxicology, 7(2), 182–190.
27. Iravani, S. (2011). Green synthesis of metal nanoparticles using plants. Green Chemistry, 13(10), 2638–2650.
28. Rajakumar, G., Gomathi, T., Thiruvengadam, M., Kalpana, V. N., & Chung, I. M. (2016). Green approach for synthesis of bioinspired zinc oxide nanoparticles for antibacterial and photocatalytic applications. Materials Science in Semiconductor Processing, 57, 233–241.
29. Ramesh, M., Anbuvannan, M., & Viruthagiri, G. (2014). Green synthesis of ZnO nanoparticles using Solanum nigrum leaf extract and their antibacterial activity. Spectrochimica Acta Part A: Molecular and Biomolecular Spectroscopy, 136, 864–870.
30. Singh, J., Dutta, T., Kim, K. H., Rawat, M., Samddar, P., & Kumar, P. (2018). 'Green' synthesis of metals and their oxide nanoparticles: applications for environmental remediation. Journal of Nano biotechnology, 16(1), 84.